Enhanced far-infrared absorption in $CePd_3$ and $YbCu_2Si_2$. II. Infrared-active optic phonons in metals

L. J. Sham
Department of Physics, University of California—San Diego, La Jolla, California 92093

J. W. Wilkins
Laboratory of Atomic and Solid State Physics, Cornell University, Ithaca, New York 14853
(Received 23 April 1984)

Zone-center optic phonons in a metal can be observed by the far-infrared absorptivity. A procedure for precisely estimating the intensity and line shape of these optic phonons is given.

I. INTRODUCTION

There have been very few observations of optic modes in metals. The bulk of the theory and data is for doped semiconductors.[1] Principally the concern has been with the effect of doping (i.e., increased screening) to decrease the Lyddane-Sachs-Teller splitting of the transverse and optical modes. It has, however, been noted[2] that the relative contribution of the optical phonons to the far-infrared (FIR) absorptivity should increase with the resistivity of the metals. Our interest has been motivated by the recent observation that some optic modes of $CePd_3$ have been seen in a FIR measurement.[3] Here we show that the strength of the optic mode in the FIR depends on the relative magnitude of phonon and electronic contributions to the dielectric function $\epsilon(\omega)$. These relative magnitudes vary with crystal structure and associated phonons and with the nature of electronic scattering processes. In many metallic compounds some of the $\vec{q}=\vec{0}$ or zone-center optic modes should be observable in the FIR.

While much of the analysis in this paper applies to all metals, we will specifically analyze the case of a valence fluctuator $CePd_3$, whose FIR spectrum stimulated this work. When the spectrum (see Fig. 1) was originally published,[3] the two features at 14.7 and 21.6 meV were not attributed to optical phonons. The principal reason for this was that the preliminary measurements[4,5] have given a zone-center transverse optic phonon at 13.5 and 17.5 meV—i.e., there was nothing at 22 meV. In addition, the measured shape of the features was different from that expected for phonons.[5] One of the points of this paper is to demonstrate how the electronic contribution to $\epsilon(\omega)$ can distort the phonon line shape. Nonetheless, there is no doubt that the two features are due to phonons. Recent measurements[6] of the room-temperature phonons of $CePd_3$ (see Fig. 2) reveal that three zone-center optic modes (each mode actually consists of two transverse

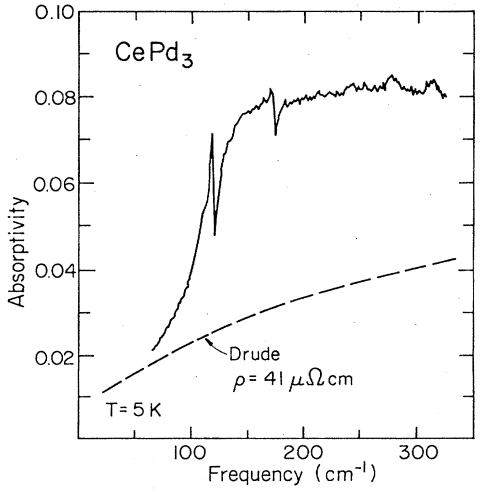

FIG. 1. Absorptivity of $CePd_3$. Note the well-resolved features at 15 and 22 meV. The dashed line is a plot of the absorptivity using the measured dc resistivity. These curves are taken from Ref. 4.

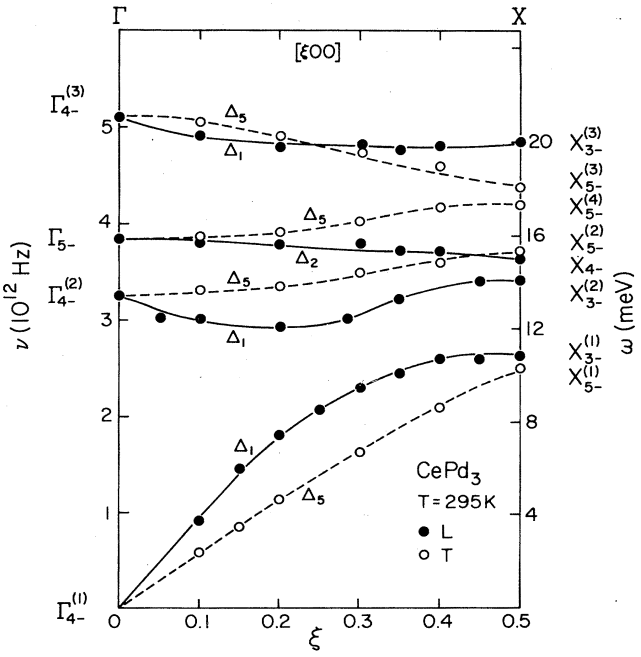

FIG. 2. Phonon spectrum of $CePd_3$ along Δ (from point Γ to point X) at room temperature. These curves are taken from Ref. 6.

modes and one longitudinal mode) are at 13.4, 15.9, and 21.2 meV. Furthermore, our analysis (see Sec. III A) shows that the middle mode is not infrared active. The slight difference between the measured energies at room temperature (13.4 and 21.2 meV) and the position of the features at 4.2 K (14.7 and 21.6 meV) may be due to temperature dependence of the phonon spectrum.

The plan of this paper is as follows. Section II contains the general theoretical approach for decomposing the dielectric function in terms of the electronic and phonon contribution. Details on the phonon terms are in Sec. III. In the following paper this analysis is applied to fit the phonon features in the absorptivity of $CePd_3$.

II. GENERAL ANALYSIS OF SURFACE ABSORPTIVITY IN THE FIR

A. Relation of absorptivity to the dielectric constant

The absorptivity $A(\omega)$ of a surface is the fraction of incident power absorbed on a single reflection. For the case of normal incidence,

$$A \simeq 4r \ , \tag{2.1}$$

where r is the real part of the reduced surface impedance

$$Z(\omega)=r+ix=[\mu(\omega)/\epsilon(\omega)]^{1/2} \ . \tag{2.2}$$

Here $\epsilon(\omega)$ and $\mu(\omega)$ are the dielectric function and magnetic permeability, respectively, of the material. For nonmagnetic metals, $\mu(\omega)\simeq 1$ and we will neglect it henceforth.

The analysis of the experiment[7] is only slightly more complicated. In particular the radiation inside the sample cavity is effectively incident at all angles. To within a few percent the angle-averaged absorptivity in the FIR (where $r\sim |x| \sim 10^{-2}$) is given by

$$A=4r[\tfrac{4}{3}+c(r)] \ , \tag{2.3}$$

where the correction $c(r)\simeq r(2\ln r - 0.5)$.

B. Connection of $\epsilon(\omega)$ to density-density correlation function

In general the dielectric function depends on wave vector $\vec{q}$ and frequency ω. However, in FIR $(q/2\pi)\sim 10^2$ cm^{-1} which is very small compared to typical electron wave numbers (approximately 10^8). Accordingly, we want the $\vec{q}\to\vec{0}$ limit of the dielectric function.

In a metal (or any crystalline solid) the dielectric function is more complicated than for isotropic media. In general,[8] an external potential $\phi_{\rm ext}$ will induce a density

$$n_{\rm ind}(\vec{r},t)=\int d^3r'\,dt'\,\chi(\vec{r},\vec{r}';t-t')\phi_{\rm ext}(\vec{r}',t') \ , \tag{2.4}$$

where $\chi(\vec{r},\vec{r}';\tau)$ is a density-density correlation. The induced density generates a potential via Poisson's equation

$$\nabla^2\phi_{\rm ind}(\vec{r},t)=-4\pi e^2 n_{\rm ind}(\vec{r},t) \ , \tag{2.5}$$

where e is the magnitude of the electron charge. Both (2.4) and (2.5) are easily solved by taking Fourier transforms. In particular the effective potential $\phi_{\rm eff}=\phi_{\rm ext}+\phi_{\rm ind}$ is given by

$$\phi_{\rm eff}(\vec{q}+\vec{G},\omega)=\sum_{\vec{G}'}\epsilon^{-1}(\vec{q}+\vec{G},\vec{q}+\vec{G}';\omega) \times\phi_{\rm ext}(\vec{q}+\vec{G}',\omega) \ , \tag{2.6}$$

where the inverse dielectric matrix is

$$\epsilon^{-1}(\vec{q}+\vec{G},\vec{q}+\vec{G}';\omega) =\delta_{\vec{G},\vec{G}'}+v(\vec{q}+\vec{G})\chi(\vec{q}+\vec{G},\vec{q}+\vec{G}';\omega) \tag{2.7}$$

and the Coulomb interaction is

$$v(\vec{q}+\vec{G})=4\pi e^2/|\vec{q}+\vec{G}|^2\Omega \ , \tag{2.8}$$

where Ω is the volume of the system. In Eqs. (2.6)—(2.8) the wave vector $\vec{q}$ is restricted to the first Brillouin zone prescribed by the reciprocal-lattice vectors $\vec{G}$.

The macroscopic dielectric function $\epsilon(\omega)$ is the inverse of the $\vec{q}\to 0$ limit of the element of the inverse dielectric matrix (2.7) with $\vec{G}=0$ and $\vec{G}'=0$. This limit is readily taken by defining a particular irreducible density-density correlation factor $\hat{\chi}(\vec{q}+\vec{G},\vec{q}+\vec{G}';\omega)$ such that $\hat{\chi}$ does *not* contain $v(q)$ as a *factor*. This definition singles out the $\vec{G}=\vec{G}'=\vec{0}$ term. Then it follows that χ satisfies[9]

$$\chi(\vec{q}+\vec{G},\vec{q}+\vec{G}';\omega)=\hat{\chi}(\vec{q}+\vec{G},\vec{q}+\vec{G}';\omega) +\hat{\chi}(\vec{q}+\vec{G},\vec{q};\omega)v(\vec{q})\chi(\vec{q},\vec{q}+\vec{G}';\omega) \ . \tag{2.9a}$$

In particular (2.9a) implies that

$$\chi(\vec{q},\vec{q};\omega)=\hat{\chi}(\vec{q},\vec{q};\omega)/[1-v(\vec{q})\hat{\chi}(\vec{q},\vec{q};\omega)] \ . \tag{2.9b}$$

The $\vec{q}\to 0$ limit immediately follows,

$$\epsilon(\omega)=1-\lim_{\vec{q}\to\vec{0}} v(\vec{q})\hat{\chi}(\vec{q},\vec{q};\omega) \ , \tag{2.10}$$

where we understand $\epsilon(\omega)$ to be the macroscopic dielectric function, i.e., the inverse of the $\vec{q}\to 0$ limit of $\epsilon^{-1}(\vec{q},\vec{q};\omega)$. Since in defining $\hat{\chi}$ we have explicitly removed the long-range interaction $v(\vec{q})$, it follows that $\hat{\chi}$ does not contain any long-range potential and hence should be well-behaved as $\vec{q}\to 0$.

In Secs. II C and II D we shall work out the lattice and electronic contribution to $\hat{\chi}(\vec{q},\vec{q};\omega)$. For simplicity, we neglect the electron renormalization of the lattice charge and the phonon effect on the electron conductivity. Then

$$\hat{\chi}=\hat{\chi}_{\rm ph}+\hat{\chi}_{\rm el} \ . \tag{2.11}$$

C. Ion charge and phonon propagators

In discussing phonons we use standard notation.[10,11] The position of the κth atom in the lth unit cell is

$$\vec{R}_{l\kappa}=\vec{x}_{l\kappa}+\vec{u}_{l\kappa} \ , \tag{2.12}$$

where any equilibrium positions

$$\vec{x}_{l\kappa}=\vec{x}_l+\vec{x}_\kappa$$

are the sums of a vector $\vec{x}_l$ defining the Bravais lattice and of $\vec{x}_\kappa$ giving the relative position of the atoms inside

the unit cell.

The displacement from the equilibrium position $\vec{x}_{l\kappa}$ is called $\vec{u}_{l\kappa}$ and can be written in terms of normal-mode coordinates,

$$\vec{u}_{l\kappa}=\left[\frac{\hbar}{NM_\kappa}\right]^{1/2}\sum_{\vec{q},j}e^{i\vec{q}\cdot\vec{x}_{l\kappa}}\vec{e}(\kappa\mid\vec{q},j)u_{\vec{q}j}\,, \tag{2.13}$$

where M_κ is the mass of the κth atom and N is the number of unit cells in volume Ω; the density of ions $n_I=n/\Omega$. The jth normal mode with wave vector $\vec{q}$ has frequency $\omega_{\vec{q}j}$, amplitude $u_{\vec{q}j}$, and an orthonormal eigenvector $\vec{e}(\kappa\mid\vec{q},j)$ associated with the κth atom.

To calculate $\hat{\chi}_{\rm ph}(\vec{q},\vec{q};\omega)$ requires the Fourier transform of that part of the ion density associated with lattice motion. Since we are interested only in the long-wavelength part (i.e., $\vec{q}\to\vec{0}$) we can approximate the ions by point charges

$$n_{\rm ion}(\vec{r})=\sum_{l,\kappa}Z_\kappa\delta(\vec{r}-\vec{R}_{l\kappa})\,, \tag{2.14}$$

where Z_κ is the charge of the κth ion. The Fourier transform of the ion density can be decomposed as

$$n_{\rm ion}(\vec{q})=n_{\rm static}(\vec{q})+n_{\rm ph}(\vec{q})\,,$$

where

$$n_{\rm static}(\vec{q})=N\delta_{\vec{q},\vec{0}}\sum_\kappa Z_\kappa e\,, \tag{2.15}$$

and to first order in the lattice displacement

$$n_{\rm ph}(\vec{q})=\sum_{l,\kappa}Z_\kappa e^{i\vec{q}\cdot\vec{x}_{l\kappa}}(-i)(\vec{q}\cdot\vec{u}_{l\kappa})\,. \tag{2.16}$$

The phonon density (2.16) can be reduced by the use of (2.13) to

$$n_{\rm ph}(\vec{q})=\sum_j Z(\vec{q},j)u_{\vec{q}j}\,, \tag{2.17}$$

where the effective charge $Z(\vec{q},j)$ is

$$Z(\vec{q},j)=-i\sum_\kappa Z_\kappa\left[\frac{\hbar N}{M_\kappa}\right]^{1/2}\vec{q}\cdot\vec{e}(\kappa\mid\vec{q},j)\,. \tag{2.18}$$

The calculation of $\hat{\chi}_{\rm ph}(\vec{q},\vec{q};\omega)$ reduces to

$$\hat{\chi}_{\rm ph}(\vec{q},\vec{q};\omega)=\frac{1}{\hbar}\sum_j|Z(\vec{q},j)|^2\hat{D}(\vec{q},j;\omega)\,, \tag{2.19}$$

where $\hat{D}$ is the short-range part of the Fourier transform of $\langle T[u_{\vec{q}j}(t)u_{\vec{q}j}(0)]\rangle$, i.e., of the phonon propagation $D(\vec{q},j;\omega)$. The general form for D is

$$D(\vec{q},j;\omega)=\frac{1}{\omega(\omega+i\gamma_{\vec{q}j})-\omega_{\vec{q}j}^2}\,, \tag{2.20}$$

where $\gamma_{\vec{q}j}$ gives the damping of the phonon modes. The phonon frequencies $\omega_{\vec{q}j}$ result from diagonalizing the dynamic matrix $\Phi(\vec{q}',\kappa,\kappa')$. To calculate $\hat{D}$ we need $\hat{\Phi}$. Fortunately it has been shown[9] that

$$\lim_{q\to0}\hat{\Phi}(\vec{q};\kappa,\kappa')=\Phi(\vec{q}=\vec{0};\kappa,\kappa') \tag{2.21}$$

holds for metals. In other words, at $\vec{q}=\vec{0}$ we can use D for $\hat{D}$.

W now have all the components to calculate the phonon contribution to the dielectric constant,

$$[\epsilon(\omega)]_{\rm ph}=-\lim_{\vec{q}\to\vec{0}}[v(\vec{q})\hat{\chi}_{\rm ph}(\vec{q},\vec{q};\omega)]=-\lim_{\vec{q}\to\vec{0}}\sum_j\frac{N}{\Omega}\frac{4\pi e^2}{\omega(\omega+i\gamma)-\omega_{qj}^2}\left[\sum_\kappa\frac{Z_\kappa}{\sqrt{M_\kappa}}\frac{\vec{q}\cdot\vec{e}(\kappa\mid\vec{q},j)}{q}\right]^2$$
$$=-\sum_j\frac{\Omega_j^2}{\omega(\omega+i\gamma_j)-\omega_j^2}\,. \tag{2.22}$$

Here ω_j are zone-center phonon frequencies and

$$\Omega_j^2=4\pi n_I e^2\left[\sum_\kappa\frac{Z_\kappa}{\sqrt{M_\kappa}}\hat{q}\cdot\vec{e}(\kappa\mid\vec{0},j)\right]^2 \tag{2.23}$$

are the effective ion plasma frequencies for zone-center phonons. Equations (2.22) and (2.23) are the central results in this paper. In Sec. III Ω_j^2 is evaluated for various cases; in particular it is nonzero for only those modes that are infrared active. The special case of $CePd_3$ is also addressed in Sec. III where a force-constant model is fitted to the measured phonon frequencies. The resulting polarization for the zone-center FIR active modes is used to evaluate Ω_j^2 via (2.23) and hence to deduce the intensities of the phonon features in FIR absorptivity.

D. Electronic part of $\epsilon(\omega)$

The electronic part of $\epsilon(\omega)$ for metals is very familiar. If $\sigma(\omega)$ is the ac electrical conductivity then

$$[\epsilon(\omega)]_{\rm el}=1+\frac{4\pi i\sigma(\omega)}{\omega}\,. \tag{2.24}$$

As an example, consider the Drude model in which a single, constant relaxation time τ characterizes the scattering of the electrons. The Drude ac conductivity is

$$\sigma_D(\omega)=\frac{ne^2/m}{\frac{1}{\tau}-i\omega}=\frac{\omega_p^2/4\pi}{\frac{1}{\tau}-i\omega}\,, \tag{2.25}$$

where n is the density of conduction electrons and ω_p the electronic plasma frequency. If this is the sole contribution to $\epsilon(\omega)-1$ then the surface impedance (2.2) reduces to

$$Z_D=r_D+ix_D=\left[\frac{\omega}{2\omega_p^2\tau}\right]^{1/2}(1-i)\,. \tag{2.26}$$

Accordingly the absorptivity for the Drude model would

increase with the square root of ω. This behavior is shown by the dashed line in Fig. 1 where the relaxation time used is that appropriate for the dc resistivity. Clearly we need to enhance the overall absorptivity. A possible model for doing this which is relevant for a valence fluctuator is discussed in the following paper.

E. General discussion of phonon line shape

For the purposes of discussing the phonon line shape we can concentrate on the frequency region within a few decay widths of zone-center phonons. In that narrow frequency range we approximate the electronic contribution to $\epsilon(\omega)$ by a constant. We define a reduced frequency

$$\nu=(\omega-\omega_j)/\gamma_j$$

and a dimensionless amplitude $\alpha=\Omega_j^2/\omega_j\gamma_j$. Then the dielectric constant can be written

$$\epsilon(\omega)=\frac{1}{r^2(1+i\zeta)^2}-\frac{\alpha}{2\nu+i}\,, \tag{2.27}$$

where $r(1+i\zeta)$ is surface impedance due to the electrons at $\omega=\omega_j$. (Note: $\zeta\simeq-1$ for the Drude model.) Then, for simplicity, supposing that $\alpha r^2\ll 1$, we can immediately write the absorptivity (2.1),

$$\tfrac{1}{4}A=r\left[1+\tfrac{1}{2}(\alpha r^2)\left[\frac{2\nu(1-3\zeta^2)+\zeta(3-\zeta^2)}{4\nu^2+1}\right]\right], \tag{2.28}$$

where the second term is that due to the zone-center phonon. In Fig. 3 a typical plot of the quantity in the large parentheses is in units of ζ^2 versus ν. The ratio of the two

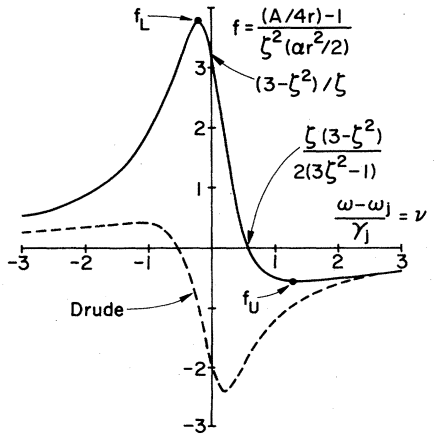

FIG. 3. Typical plot of normalized contribution of an optic phonon to the absorptivity as a function of renormalized frequency $\nu=(\omega-\omega)j/\gamma_j$. Note that four characteristic points all of which depend on the ratio $\zeta=x/r$: the two extrema f_L and f_U, the value at the resonance frequency ($\nu=0$) and the zero crossing. The dashed curve is for the Drude conductivity in which $\zeta\simeq-1$.

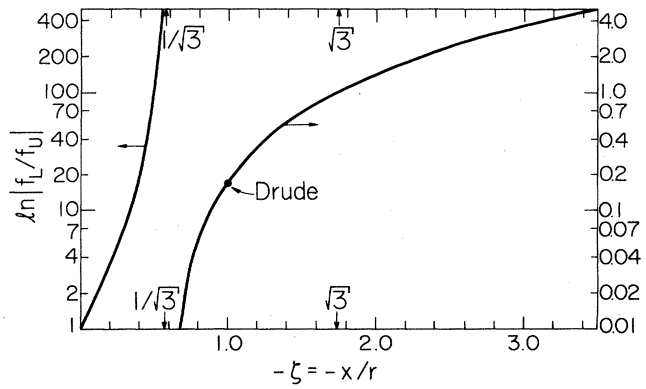

FIG. 4. Plot of f_L/f_U defined in Fig. 3 for $-\zeta=-x/r$. Note the Drude value $\zeta=-1$.

extrema (f_L/f_u) is plotted in Fig. 4 as a function of the ratio of the imaginary part of the surface impedance to the real part ($\zeta=x/r$). For comparison the Drude values are specifically indicated. Clearly the Drude value of r and x will not explain the shape of the phonon features seen in $CePd_3$ (Fig. 1).

III. PROPERTIES OF INFRARED-ACTIVE PHONONS

In this section we first survey the infrared- and Raman-active modes and then analyze the phonons of $CePd_3$ to calculate the relevant Ω_j^2.

A. Infrared- and Raman-active optic modes

We start by remembering that the contribution of a zone-center phonon ω_j to $\epsilon(\omega)$ is proportional to an effective ion plasma frequency

$$\Omega_j^2=4\pi n_I e^2\left[\sum_\kappa Z_\kappa\hat{q}\cdot\vec{e}(\kappa\,|\,\vec{0},j)/\sqrt{M_\kappa}\right]^2. \tag{3.1}$$

For the large parentheses to be nonzero it must be invariant under the transformation of the space group of any specific crystal structure. Within the large parentheses we see that $\hat{q}$ transforms like a vector, while each $\vec{e}(\kappa\,|\,\vec{0},j)$ belongs to an irreducible representation of the point group of Γ. But if the scalar product $\hat{q}\cdot\vec{e}$ is to be invariant, then *only those* $\vec{e}$ *that transform like vectors are infrared active.*[12] For cubic crystals those modes are Γ_{4-}, Γ_{15}, or T_{1u}, depending on which notation[13–16] is employed. A similar analysis can be done for the Raman-active modes. Table I contains a listing of the zone-center phonon modes according to activity for several crystal structures relevant for valence fluctuators.

B. Application to $CePd_3$

To calculate Ω_j^2 for the infrared-active modes, we need to determine the polarization vector $\vec{e}(\kappa\,|\,\vec{0},j)$. This is achieved by constructing a force-constant model fitted to the phonon frequencies measured by neutron scatterings.

$CePd_3$ has the Cu_3Au structure which is a simple cubic

TABLE I. Optical modes in valence fluctuators.

Structure[a]	Space group[a]	Valence Fluctuators	Acoustic[a]	Infrared[a]	Raman[a]	Other optical modes[a]
$ThCr_2Si_2$	$I4/mmm$ (D_{4h}^{17}) tetragonal	$CeCu_2Si_2$ $EuCu_2Si_2$ $YbCu_2Si_2$	$\Gamma_{3-}+\Gamma_{5-}$	$2\Gamma_{3-}+2\Gamma_{5-}$	$\Gamma_{1+}+\Gamma_{2+}$ $+2\Gamma_{5+}$	
Cu_3Au	$Pm3m$ (O_h^1) cubic	$CePd_3$, $CeSn_3$ $YbAl_3$, $YbIn_3$	Γ_{4-}	$2\Gamma_{4-}$		Γ_{5-}
CaB_6	$Pm3m$ (O_h^1) cubic	SmB_6	Γ_{4-}	$2\Gamma_{4-}$	$\Gamma_{1+}+\Gamma_{3+}$ $+\Gamma_{5+}$	$\Gamma_{4+}+\Gamma_{5-}$
NaCl	$Fm3m$ (O_h^5) cubic	CeN, CeP, SmS Smse, SmTe, TmSe, TmTe, YbS YbSe, YbTe	Γ_{4-}	Γ_{4-}		
NaZ_{13}	$Fm3c$ (O_h^6) cubic	$CeBe_{13}$	Γ_{4-}	$6\Gamma_{4-}$	$2\Gamma_{1+}+4\Gamma_{3+}$ $+4\Gamma_{5+}$	$2\Gamma_{2+}+5\Gamma_{4+}+\Gamma_{1-}$ $+\Gamma_{2-}+2\Gamma_{3-}+6\Gamma_{5-}$
$MgCu_2$	$Fd3m$ (O_h^7) cubic	$EuRh_2$ $YbAl_2$	Γ_{4-}	$2\Gamma_{4-}$	Γ_{5+}	$\Gamma_{2-}+\Gamma_{3-}+\Gamma_{5-}$

[a]Reference 13.

lattice with four atoms per unit cell: Ce at the corners of the cube and Pd at the face centers: $\kappa=0$ denotes the Ce atom in the unit cell and $\kappa=1,2,3$ designate the Pd atoms on the x,y,z planes, respectively. At the Brillouin-zone center, $\vec{q}=\vec{0}$, the dynamical matrix $\Phi_{\alpha\alpha}(\kappa,\kappa')$ has, from symmetry considerations, only four independent elements: $\Phi_{xx}(1,1)$, $\Phi_{yy}(1,1)$, $\Phi_{xx}(1,2)$, and $\Phi_{zz}(1,2)$. The other elements are either zero or may be obtained from these four by a point-group operation or by infinitesimal translational invariance. However, these four force constants are determined by only three nonzero phonon frequencies at $\vec{q}=\vec{0}$.

An additional assumption of nearest-neighbor force constants for phonons at X, zone boundary in the $\langle 100\rangle$ direction, yields

$$\omega^2(X_{3-})-\omega^2(X_{4-})=\Phi_{zz}(12) \tag{3.2}$$

for one of three X_{3-} modes. There is only one X_{4-} mode. Identification of this X_{3-} with the highest measured $X_{3-}^{(3)}$ mode leads to complex force constants. Identification with the lowest measured $X_{3-}^{(1)}$ mode yields two possible sets of force constants. The ambiguity is resolved by the reasonable choice that the higher-lying mode $\Gamma_{4-}^{(2)}$ corresponds to mainly Pd atoms vibrating against one another while the lower-lying mode $\Gamma_{4-}^{(1)}$ corresponds to Ce beating against the Pd atoms.

The calculation of Ω_j^2 proceeds as follows. Since the two transverse and longitudinal zone-center modes of any symmetry are degenerate in a metal, we can arrange for the polarizations of these modes to be parallel to three crystal axes; thus only one set of polarizations is required to calculate Ω_j^2. We choose the charge of Pd and Ce to 10 and 3.45, respectively, the latter number reflecting the valence-fluctuating character of Ce. Then we found $\Omega^2(\Gamma_4^{(2)})=4600$ meV^2 and $\Omega^2(\Gamma_4^{(3)})=420$ meV^2. (If, as our fourth condition, we had chosen the difference of the zone-boundary frequency X_4 and the higher-lying $X_{3-}^{(3)}$, then we would have obtained 4400 and 610, respectively.)

IV. CONCLUSIONS

We have shown that the absorptivity can be calculated, via (2.3) and (2.2), using

$$\epsilon(\omega)=1+\frac{4\pi i\sigma(\omega)}{\omega}-\sum_j \frac{\Omega_j^2}{\omega(\omega+i\gamma_j)-\omega_j^2}\ , \tag{4.1}$$

where the zone-boundary phonons ω_j can be taken from experiment. The calculation of Ω_j^2, via (2.23), depends on the crystal structure and the phonon dispersion. In the next paper[17] we shall consider a model for $\sigma(\omega)$ which has a reasonable fit for all features of the absorptivity of $CePd_3$. Finally we would stress this central point: optic modes in metals are observable in the FIR.

ACKNOWLEDGMENTS

We have benefited from discussions with Al Sievers, Dan Cox, Fred Pinkerton, and Charbel Tannous. One of us (L.J.S.) wishes to thank Professor N. W. Ashcroft and his colleagues for the hospitality of the Laboratory of Atomic and Solid State Physics where this work was performed during a sabbatical leave. This work was supported in part by the National Science Foundation under Grants No. DMR-80-18440 (L.J.S.) and No. DMR-83-14764 (J.W.W.).

[1](a) Early theoretical work on the screening of the longitudinal optic phonons can be found in V. L. Gurevich, A. I. Larkin, and Yu. A. Firsov, Fiz. Tverd. Tela. (Leningrad) **4**, 185 (1962) [Sov. Phys.—Solid State **4**, 131 (1962)]; B. B. Vargas, Phys. Rev. **137**, A1896 (1965); W. Cochran, R. A. Cowler, G. Dolling, and M. M. Elcombe, Proc. R. Soc. London, Ser. A **293**, 433 (1966); (b) the first experimental verification can be found in A. Mooradian and A. L. McWhorter, Phys. Rev. Lett. **19**,

849 (1967).
[2]I. P. Ipatova, A. A. Maradudin, and D. L. Mills, Solid State Commun. **8**, 561 (1970).
[3]F. E. Pinkerton, A. J. Sievers, J. W. Wilkins, M. B. Maples, and B. C. Sales, Phys. Rev. Lett. **47**, 1018 (1981).
[4]F. E. Pinkerton and A. J. Sievers, Infrared Phys. **22**, 377 (1982); F. E. Pinkerton, Ph.D thesis, Cornell University, 1981.
[5]See Sec. 46.2 of the thesis in Ref. 4.
[6]We are indebted to C. Stassis for allowing us to use Fig. 2 prior to publication.
[7]See Sec. 2.C of Ref. 4 for a detailed analysis.
[8]Here we follow the approach and notation of W. Hanke and L. J. Sham, Phys. Rev. B **12**, 4501 (1975) and Ref. 9.
[9]L. J. Sham, Phys. Rev. B **6**, 3581 (1972).
[10]A. A. Maradudin, E. W. Montroll, G. H. Weiss, and I. P. Ipatova, *Theory of Lattice Dynamics in the Harmonic Approximation,* 2nd ed. Solid State Physics Suppl. No. 3 (Academic, New York, 1971).
[11]M. Born and K. Huang, *Dynamical Theory of Crystal Lattices* (Oxford University Press, London, 1954).
[12]See, for example, p. 414f. of Ref. 10.
[13]S. C. Miller and W. F. Love, *Tables of Irreducible Representations of Magnetic Space Groups* (Pruett, Boulder, 1967).
[14]G. F. Koster, J. O. Dimmock, R. G. Wheeler, and H. Statz, *Properties of 32 Point Groups* (MIT Press, Cambridge, 1963); G. F. Koster, Solid State Phys. **5**, 173 (1957).
[15]M. Tinkham, *Group Theory and Quantum Mechanics* (McGraw-Hill, New York, 1964).
[16]*International Tables for X-ray Crystallography* (Kynoch, Birmingham, England, 1952).
[17]F. E. Pinkerton, B. C. Webb, A. J. Sievers, J. W. Wilkins, and L. J. Sham, following paper, Phys. Rev. B **30**, 3068 (1984).